VOL. 04 NO. 5,
MAY, 2024
E-ISSN 3027-1339
P-ISSN 3026-8257



African Scholar Publications & Research International
www.africanscholarpub.com

Journal of Systematic, Evaluation and Diversity Engr. (JSEDE)

MECHANICAL PROPERTIES AND MICROSTRUCTURAL CHARACTERISTICS OF MARTENSITIC STEEL DEVELOPED VIA THERMAL CYCLING TREATMENT

Ologunye, O. B.[1]; Oyetunji, A.[2]; Olaniran, O.[2]; & Daramola, O. O.[2]

[1]Department of Mechanical Engineering, Federal Polytechnic Ede, Osun State, Nigeria. [2]Department of Metallurgical and Materials Engineering, Federal University of Technology Akure, Ondo State, Nigeria.
opeologunye@yahoo.com

Abstract

Cyclic quenching and tempering (CQT) heat-treatment methods can improve the mechanical properties of martensitic medium carbon steel due to the development of fine grain size microstructure. To explore various avenues for enhancing steel quality, this work aims to investigate the mechanical properties and microstructural characteristics of martensitic steel developed via thermal cycling treatment. As received hot-rolled, AISI 1040 ribbed steel bars with a diameter of 12mm containing 0.35 wt% C, 0.28wt % Si and 0.62wt%Mn were first normalized in a muffle furnace at 845℃. Samples were thereafter subjected to thermal cycling at 743℃, 761℃ and 779℃ in the furnace respectively within the dual-phase region and then tempered at 450ºC. Mechanical properties of the specimens were evaluated and characterized by optical microscopy (OM). The fracture surfaces of the samples were examined using the scanning electron microscope (SEM). The results show that with an increased in lamilarization temperature at 779℃, ultimate tensile strength, yield strength, percentage elongation, and modulus of elasticity all ncreased while the

fracture strength decreased. The Optical micrographs and SEM micrographs revealed that the sample contains lath martensite and ferrite and carbide with fine grains after tempered at 450°C. These findings indicate that thermal cycling treatment is an effective method for producing high-performance martensitic steel with improved mechanical properties suitable for all industrial applications.

Keywords: Thermal, Lamilarization temperature, Micrographs, Strength, Mechanical properties, Fracture.

Introduction

Medium carbon low alloy steels are becoming more and more necessary for use in the automotive, aerospace, military, and other industries. This is because of their exceptional mechanical properties, that is high fatigue and wear resistance, and exceptional fracture toughness (Liu *et al*., 2018). These properties result from the formation of lath and retained phases in the microstructure of medium carbon low alloy steels during the heat-treatment process (Abbasi *et al*., 2018). Quenching and tempering (QT) is one of the most widely utilized heat-treatment techniques in manufacturing industries. One of the key techniques for enhancing material qualities is CQT. The development of tempering technology influences the formation of the microstructure and establishes the final mechanical properties (Shu *et al*., 2017; Wang et al., 2023). After quenching, tempering is done to achieve a balance between toughness and hardness. It affects mechanical characteristics widely, changing the microstructure from lath martensite to ferrite and carbides and decreasing brittleness and increasing toughness. In industrial applications, enhanced toughness of high strength lath martensitic structures is a key problem. According to Shu *et al*., (2017) and Wang et al., (2023), QT is main heat treatments used to provide a high combination of toughness and strength. The supersaturated phase of carbon is formed by quenching, whereas the excess carbon of the α′ phase is diffused into the retained γ phase through tempering (Tao et al., 2016). High angle grain boundaries are expected to have a major impact on the mechanical properties of steel (Wang *et al*., 2016). It has been reported that the characteristics acquired via QT techniques can be further strengthened by reducing the grain size, which is made possible by microalloying (Villalobos *et al*., 2016). Repeating QT operations is one of the most practical, easy to use, and economical heat treatment techniques. Strength, shock absorbing energy, and ductile-brittle transition temperatures (DBTT) are all significantly increased by

this grain refining. The average grain size (AGS) of a polycrystalline metal has a significant influence on its mechanical properties (Zhang *et al*., 2017). However, corrosion resistance is an essential feature when considering the actual application of carbon steels. Because of their poor corrosion resistance, carbon steels, for instance, corrode easily in the mining, petrochemical, and chemical process sectors. As a result, carbon steels require continuous replacement after some time resulting in significant maintenance cost (Loto *et al*., 2019; Majd *et al*., 2019)

Manufacturers have become more interested in the enhancement of medium carbon steel's mechanical qualities for many years. Many studies have been conducted to elucidate the mechanical behavior of medium carbon steel; they include Krauss, (2017); Krolicka *et al*., (2019); Hu *et al*., (2015); Ma *et al*., (2018), and others. The precise effect of the morphology (shape, size, and distribution) of the second-phase martensite on the microstructure and toughness of medium carbon steel is still unknown, despite the fact that this effect is thought to be extremely significant for enhancing the material properties of the steels (Krauss, 2017). Carbon content ranges from 0.25% to 0.6% in medium carbon steel. The desired properties of medium carbon steel can be obtained through heat treatment (Suresh, 2021). Carbon steel continues to be the most widely used steel despite the development of numerous alloys due to its affordability, availability, ease of protection, and variety in terms of mechanical behavior. AISI 1040 medium carbon steel is commonly used to construct carriage bolts, machine screws, crankshafts, couplings, and cold-headed parts. It can also be used for machining, tie wire, u-bolts, and concrete reinforcing rods (Unueroh *et al*., 2013). Because of their extreme strength and hardness, martensitic steels are widely used in abrasive, wear-resistant, armor, and other special-purpose steels. Complex service scenarios necessitate the improvement of martensitic steels with a variety of features. Maintaining strict control over carbon addition has been shown to be an effective tactic for improving martensite microstructures; nevertheless, there are notable drawbacks in terms of toughness, plasticity, and weldability. According to Hu *et al*., (2015), the strength and toughness of low-carbon martensitic steels can be considerably increased by the addition of second-phase martensite, which improves the interactions between dislocations and grain boundaries. Furthermore, in the coarse-grained heat-affected zone (CGHAZ), the presence of second-phase martensite at high temperatures prevents grain formation and improves the weldability of steels (Ma *et al*., 2018). Strengths above 1200 MPa can be achieved by martensite steel with 0.3% carbon content. Because of this, the iron and steel sectors are always searching for

novel approaches to control the process of improving martensitic steels' strength, toughness, and plasticity while preserving carbon content and guarantee weldability.

Other recent research on second-phase particles mostly concern the nature, amount, dimensions, and morphology of precipitates (Huihui *et al*., 2018; Lei *et al*., 2018). The strength and toughness of martensitic steel were expected to enhance with the addition of 0.09Ti to medium carbon steel. Because of improvements in the technology of steel manufacturing, there is an increasing need for high-quality steel, thus it is critical to consider all of the alternatives for improving the quality of steel. According to recent studies, by decreasing core defects and separating alloying components in different steel grades, the soft reduction (SR) technique can enhance toughness and microstructure (Ji *et al.,* 2017; An *et al*., 2019). As-quenched martensite is essential as the initial microstructure, tempering can produce a very wide range of microstructures and mechanical properties (Krauss, 2017). Research has been done on the relationship between microstructure properties and fracture toughness (Zhou *et al*., 2019; Zhou *et al*., 2020). It was proposed that the carbon content of the martensitic microstructure determines its strength (Krauss, 2016). Up to roughly 0.5 weight percent, where martensite is primarily lath martensite, the yield strength rises almost linearly with carbon content; nevertheless, the mechanism underlying this strengthening is still up for debate (Gao, *et al.,* 2019). In order to improve the design process, this work intends to examine the mechanical properties and microstructural characteristics of martensitic steel developed via thermal cycling treatment.

Experimental Procedures

Materials

As received hot-rolled, AISI 1040 ribbed steel bars with a diameter of 12mm was used for this research. The chemical composition (spectrometric analysis) of the steel shown in table 1 was determined with the aid of spectrometer and the samples were machined into various tests specimens. The carbon content from table 1 falls within the range of 0.25% – 0.6% and this qualifies it to be a medium carbon steel.

Table 1: Chemical Composition of the AISI Steel

ELEMENT	C	Si	Mn	P	S	Cr	Mo	Ni	Cu	V
CONTENT (wt%)	0.349	0.283	0.621	0.033	0.032	0.014	0.014	0.090	0.148	0.005

Cyclic Heat–Treatment

The operating temperatures for the heat treatment were determined by calculating the lower critical point, AC_1 at 725^OC and the upper critical point, AC_3 at 795^OC using Grange empirical formula as stated in equations 1 and 2. (Gorni, 2019).

$AC_1 = 1333 - 25Mn + 40Si + 42 Cr - 26 Ni$ (1)

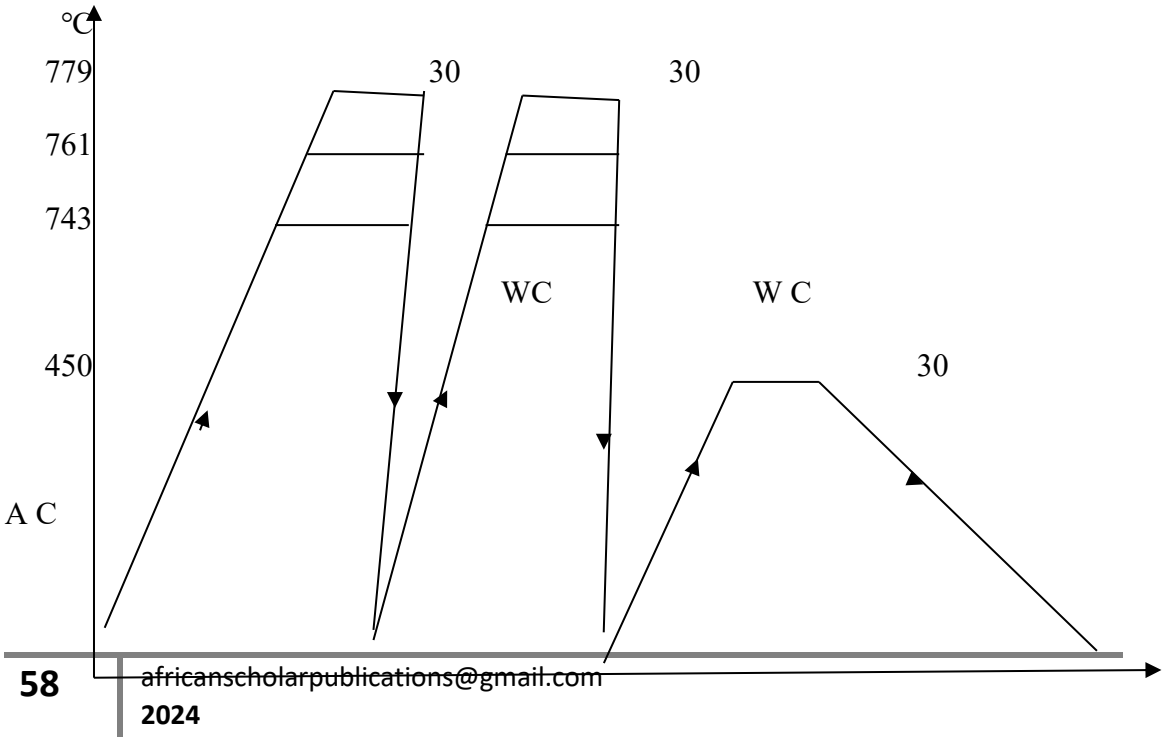
$AC_3=1570 - 323C - 25Mn + 80Si - 3Cr - 32Ni$ (2)

Martensite start temperature (Ms) and Bainite start temperature (Bs) were also determined using Grange and Stewart empirical formula, and Takada empirical formula as stated in equations 3 and 4 respectively.

Ms = 537.8 – 361.1C – 38.9 (Mn + Cr) – 19.4 Ni – 27.8 Mo = 378℃ (Gorni, 2019). (3)

Bs=1336 – 1446 C -- 62.3 Mn – 36.5 Si –47.8 Cr – 160 V – 77.5 Mo = 498℃ (Gorni, 2019) (4)

A total of forty (40) samples were used for this experiment. The steel specimens produced were first normalized at temperature of AC_3 +50℃ = 845℃ in a muffle furnace and soak for 30 minutes followed by cooling in air. Twelve (12) samples each were thereafter subjected to thermal cycling at 743℃, 761℃, 779℃ in the furnace respectively within the dual-phase region with the same holding times of 30 minutes followed by cooling in water at room temperature (25℃) and then tempered at 450ºC, for a soaking time of 30 minutes, then allowed to air cool as shown in figure 1.



Time (mins)

Figure 1: Temperature – Time Curve of Heat Treatment

Mechanical Testing

The tensile testing samples were machined into the dimensions of 50 mm gauge length, 6.5 mm gauge diameter, 30 mm fillet radius, and reduced section length of 5 mm according to the ASTME8 standard as shown in figure 2. Tensile tests were carried out on computerized Universal Instron Testing Machine (model 3369) having a capacity of 35 KN to determine the parameters showing in table 2 below. Izod impact machine was used to perform impact test on heat treated samples at room temperature to determine the performance of the developed steel. Hardness testing was carried out on brinell hardness tester (Monsanto Testing Machine Model) with samples secured in the tensiometer and compressed with a 7.5 KN force for approximately 15 seconds. An average of three readings was taken as the hardness for each sample. The indentation diameter was measured using an eyepiece and then determine the material's brinnel or hardness number by using the conversion table. The Brinell hardness (BHN) which is the pressure per unit surface area of the identification in kg per square meter is calculated as

$$W = \frac{\text{BHN}}{\left(\frac{\pi D}{2}\right)\left(D - \sqrt{D^2 - d^2}\right)}$$

Where W is load on indenter, kg,
D is diameter of steel ball, mm,
d is average measured diamerter of indentation, mm

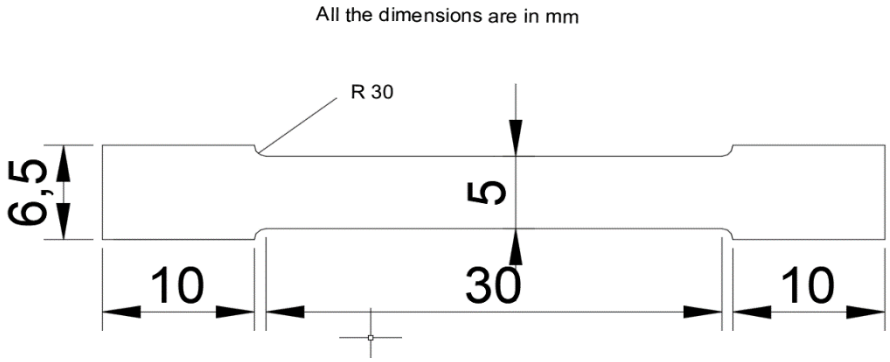


Figure 2: Tensile test sample

Microstructural Analysis

Microstructure was characterized by optical microscopy (OM) and the fracture surface of the samples was examined using the scanning electron microscope (SEM) at Obafemi Awolowo University (OAU), Ile Ife Osun State, Nigeria to observe the fracture behavior of heat–treated sample

RESULTS AND DISCUSSION

Mechanical Properties

Table 2 displays the results of the samples tested in the Universal Instron Machine, model 3369, at Obafemi Awolowo University (OAU), Ile Ife. The findings demonstrate that, with increasing lamilarization temperature, the specimens' ultimate tensile strength, yield strength, percentage elongation, and modulus of elasticity all increased while their fracture strength decreased, indicating an increase in ductility and low dislocation density that improved the tested steel's performance and formability. From the as-received sample (control), there was a 9.23% rise in UTS at 779°C, a 13.41% increase in the percentage elongation, and a 32.52% increase in the modulus of elasticity. The result also showed a 7.14% increase of UTS at 779℃ from the sample lamilarised at 743℃ and a subsequent 9.76% increase in percentage elongation as well as 26.07% modulus of elasticity. While at 779℃ , there was a 4.59% increase of UTS from the sample lamilarised at 761℃ and a subsequent 2.43% increase in percentage enlongation as well as 15.40% modulus of elasticity

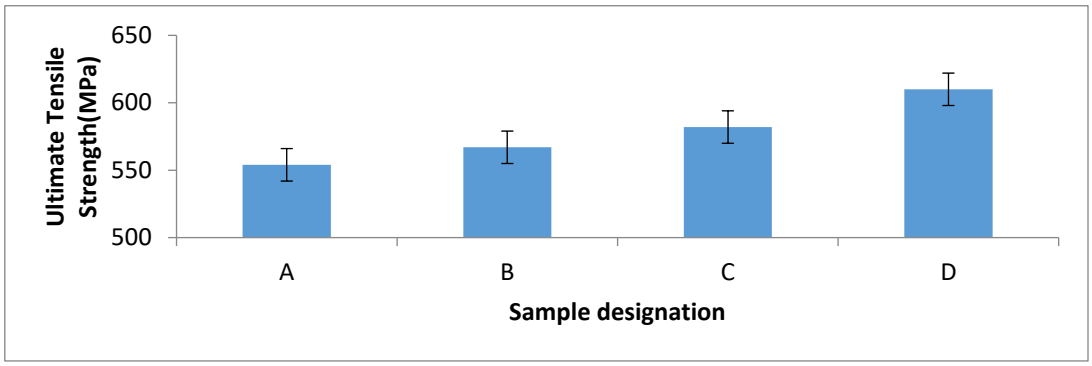
Table 2: Tensile Properties

Sample TEMP. (°C)	Length (mm)	Diameter (mm)	Tensile strain (mm/mm	Tensile extension (mm	YS (MPa)	UTS (MPa	FS (MPa	%EL	%RIA	Modulus (E modulus) (MPa)
Control, A	25.00	5.00	0.25	7.39	250.00	554.36	426.19	0.71	1.19	2249.93
743 (B)	25.00	5.00	0.23	6.46	316.66	567.12	422.63	0.74	0.67	2465.22
761 (C)	25.00	5.00	0.20	4.93	426.66	582.69	415.15	0.80	0.026	2820.95
779 (D)	25.00	5.00	0.18	5.50	433.33	610.74	405.70	0.82	0.21	3334.43

.

Figure.3a-b, show the histogram for engineering stress and strain respectively obtained from uniaxial tensile tests performed to the heat treated sample for the selected dua-phase (lamilarisation) temperatures and holding times. The ultimate tensile strength, % elongation as well as modulus of elasticity increased with heating temperature as

shown in Figure 3 a, d. As observed from these figures, all specimens exhibit a continuous yielding behaviour in spite of differences in the phase mixture obtained after the application of distinct cycling treatments. This indicates that every single specimen show a seamless change in behavior from elastic to plastic. Additionally, the average values of homogeneous hardening under strain (or "YS/UTS" ratio) for each of the heated specimens at the lamilarization temperatures are displayed in Figure.3c. This "YS/UTS" ratio indicates a material's propensity to undergo plastic deformation. All heat-treated tensile specimens exhibit a comparable capacity for strain hardening. This ratio, which ranges from 0.56 to 0.71, is consistent with Bagliani (Bagliani et al., 2013) and Mandal (Mandal et al., 2016) as typical YS/UTS ratios in multiphase steels



Fiure 3 a: Engineering Stress of the Sample

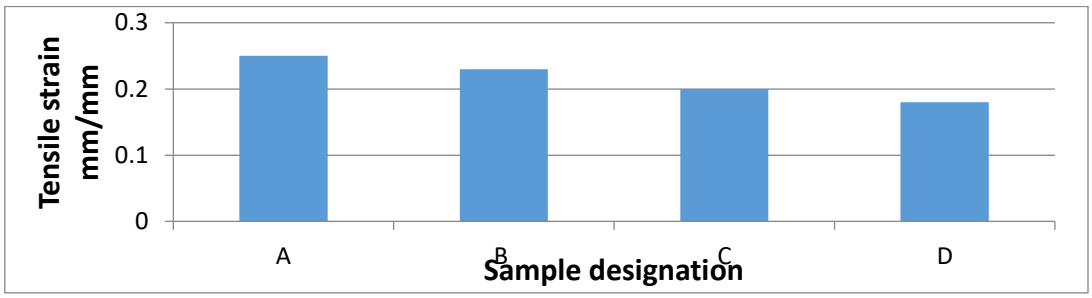


Figure 3b: Engineering Strain of the Sample

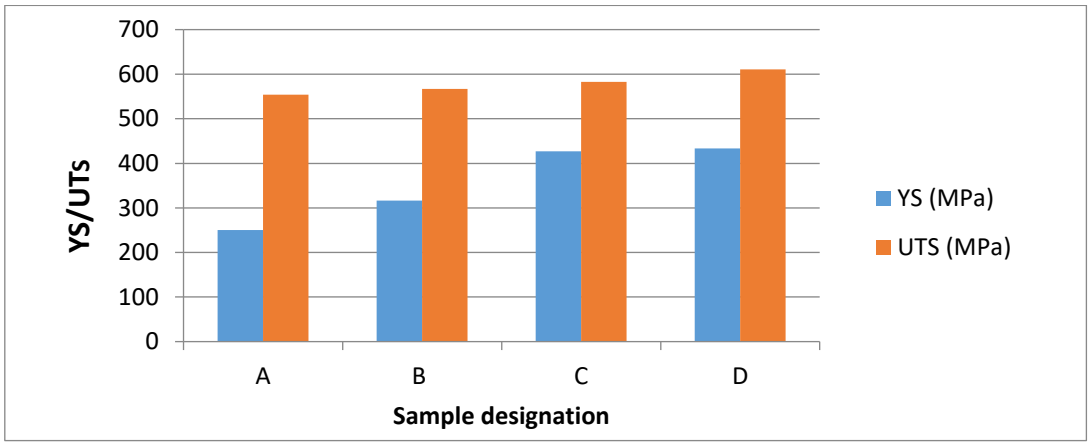


Figure 3c: YS/UTS of the Sample

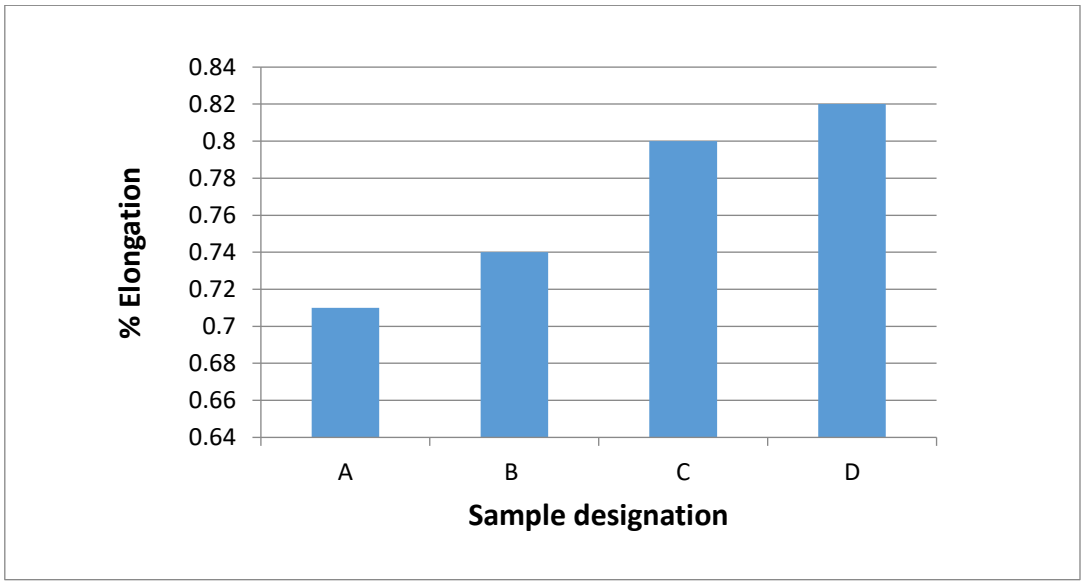


Figure 3d: Percentage Elongation of the Sample

It can also be observed from Table 3 and Figure 4a that the control sample has the lowest hardness and tempered samples have the highest hardness at 779℃. This shows that austenite transforms to martensite and the crystal structure transforms from face center cubic to body center tetragonal. It forms high dislocation density in the martensite that increases the hardness. During the tempering process, lath martensite transform to ferrite and carbides. Carbon content of martensite decreases as carbon diffuses into carbides. At the same time the internal stress will be relieved as the atoms rearrange and dislocation density is reduced. These factors cause the enhancement in mechanical properties of tested samples. Dislocation density is critical to

strengthening after all stages of tempering. It increases during strain hardening, increasing hardness and tensile strength, and rapidly decreases during tempering.

Table3: Impact and Hardness Test of the Sample

SAMPLE TEMP. ℃	Impact (Joules)	Impact strength J/mm^2	Hardness(Brinell) BHN
A- Control	51.76	2.64	93.66
B -743	59.79	2.99	137.53
C- 761	56.66	2.89	152.53
D-779	54.66	2.73	163.49

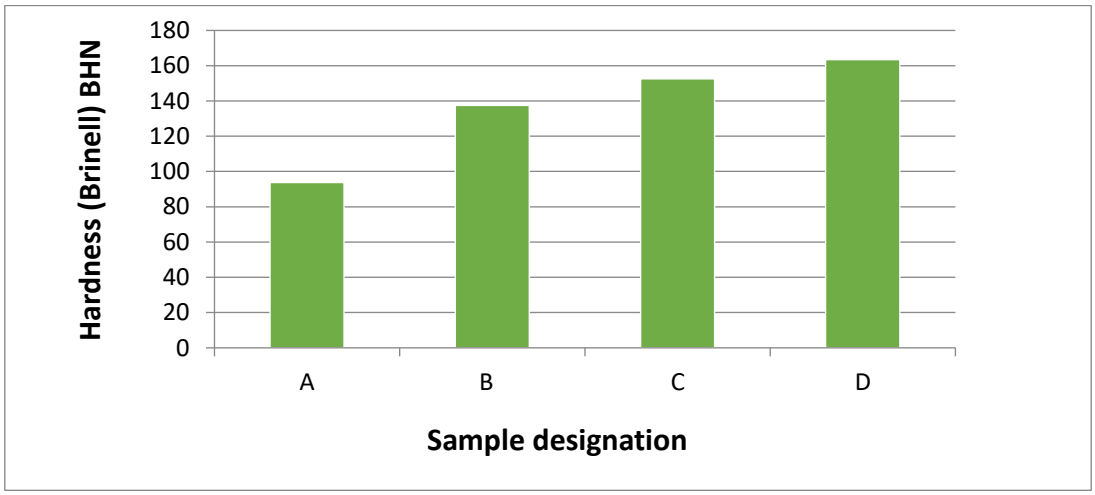


Figure 4a: Hardness of the Sample

Table 3 and Figure 4b, show that the impact strength falls as the lamilarization temperature rises because secondary fractures start to show up, indicating the occurrence of induced martensitic transformation. It was discovered that the presence of block austenite negatively affected the impact strength and grain sizes, which subsequently changed into martensite. By increasing the amount of film-like austenite, the impact strength might be raised.

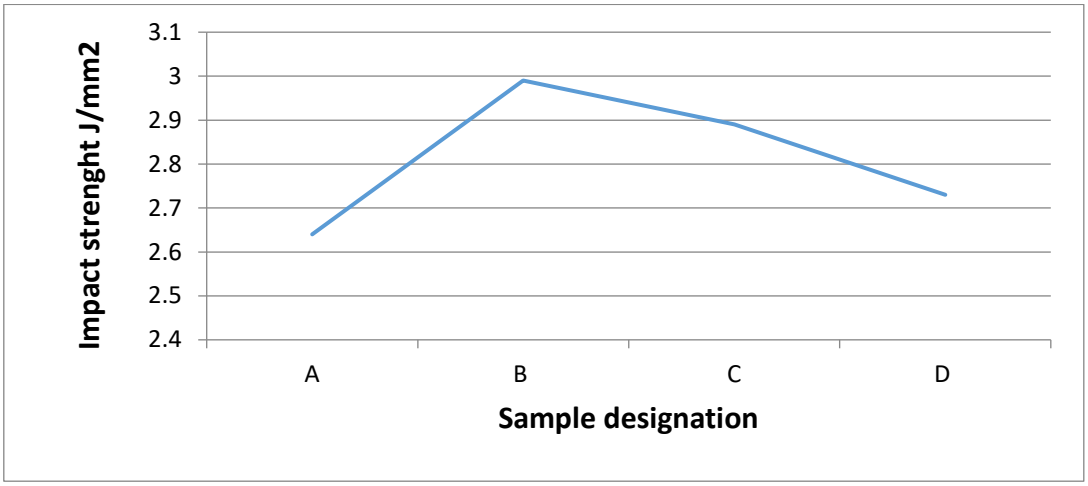


Figure 4b: Impact Strength of the Sample

Microstructural Evolution

The Optical micrographs of AISI 4040 steel normalized and tempered at 450°C is shown in Figure 5b - d. It can be observed that the samples consist of lath martensite and ferrite and carbide with fine grains. With the increasing temperature, lath martensite transform to ferrite and carbides. While Figure 5a (control) consisted of blocks lath martensite (black arrow) and retained austenite with coarse grains (blue arrow). The martensite crystals are extremely fine. Therefore, in order to transform large volumes of austenite, many crystals of martensite are necessary, producing the extremely fine crystal size of lath martensite. The large number of fine crystals means that there is a very large martensite crystal interface area associated with an as quenched martensitic microstructure. This large interfacial area would be expected to produce a strong driving force for grain growth during tempering. Dislocation density residuals at any point throughout the tempering process play a vital role in the strain hardening that resulted in the high hardness and tensile strengths of tempered martensite. Other components that may contribute to the strength of tempered martensite include precipitates and boundaries.

The amount of retained austenite was comparable when the lamilarisation temperature was in expressions of 743℃, and 761℃. In contrast, the highest concentration of austenite occurred at the highest tested temperature (779℃). However, because of the transformation-induced plasticity (TRIP) effect, which improved its elongation, it undergo martensitic transformation to a larger extent during tensile testing at higher lamilarization temperatures. Thus, by minimizing carbides in the final microstructure,

the resistance to cleavage failure and impact toughness can be enhanced. Conversely, the toughness and ductility are improved by the fine austenite films present in between the ferrite laths. Indeed, austenite films have the ability to blunt cracks. But if carbon-enriched residual austenite film disperses finely among the ferrite laths, it can boost toughness and ductility. If not, the massive blocky portions of austenite may change into coarse, brittle, untempered, and hard martensite, which could negatively impact the mechanical characteristics (Neog et al, 2021).

In general, cementite particles were clearly apparent in all of the steels upon tempering at 450°C. Cementite particles are finely dispersed throughout the ferrite grain in Figure 5b, indicating poor strength and high ductility as well as the inability to be used in load-bearing applications. Larger, less noticeable black spots in Figure 5c likely reflect second phase precipitate with some austenite still present, whereas the white color stands for ferrite. This suggests that the material is strong and ductile, making it suitable for load-bearing applications (Unueroh *et al*., 2013; Unueroh et al., 2019). With pro-eutectoid ferrite present, Figure 5a displayed a pearlitic structure. A greater portion of the sample was composed of martensite, which had a lower retained austenite percentage. Though it contains some spheroidal-shaped carbide precipitate (cementite) and lath martensite and ferrite, the bainite structure depicted in Figure 5b was coarser than that seen in Figure 5c. Martensite laths make up the steel, as seen in Figure. 5b, and the interior of the laths exhibits a higher density dislocation

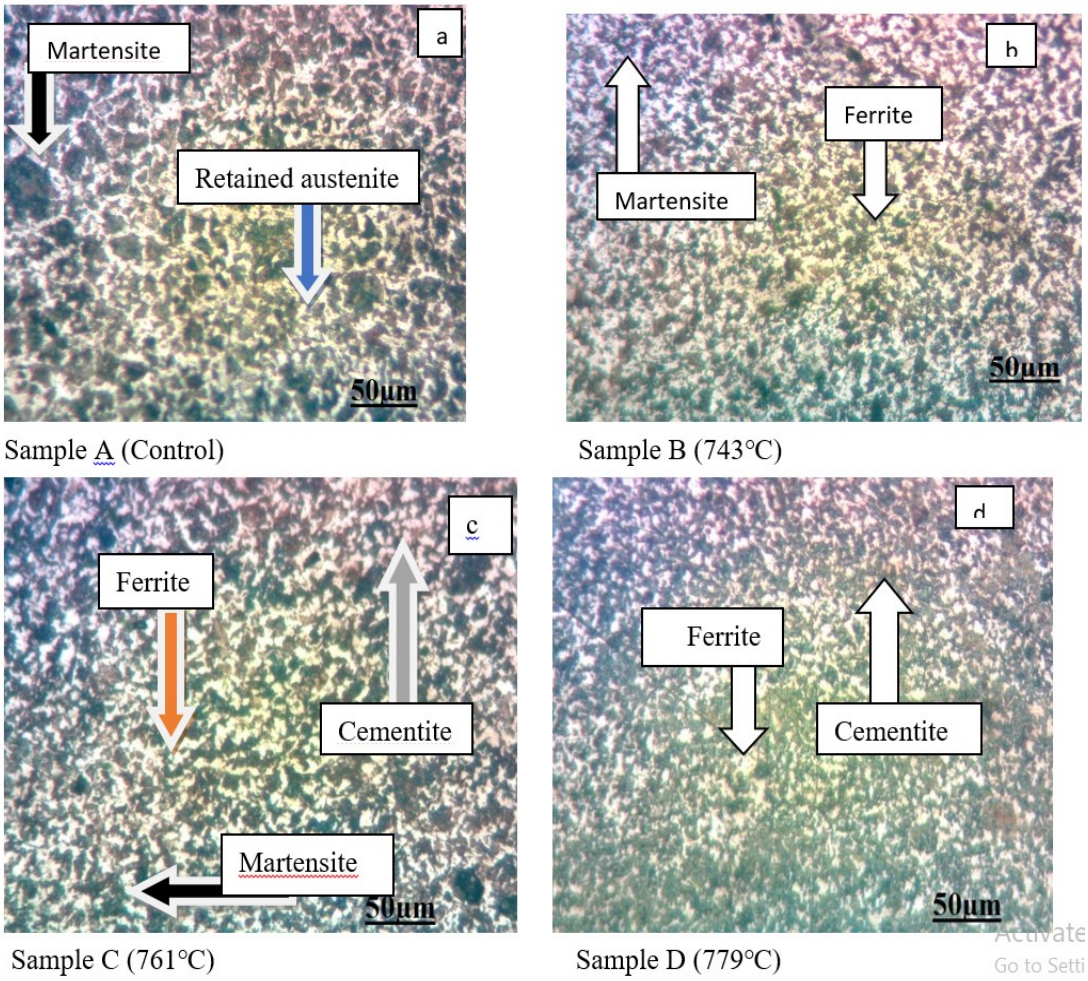


Figure 5: Optical Micrographs of Steel Sample

The SEM micrographs and corresponding EDX spectra of heat–treated samples are illustrated in Figure 6, 7, 8, 9 which are in good agreement with optical micrographs. The control samples consist of lath martensite and a small amount of retained austenite as shown in Fig.6a and spheroidal cementite in ferrite matrix with an extremely high dislocation density.

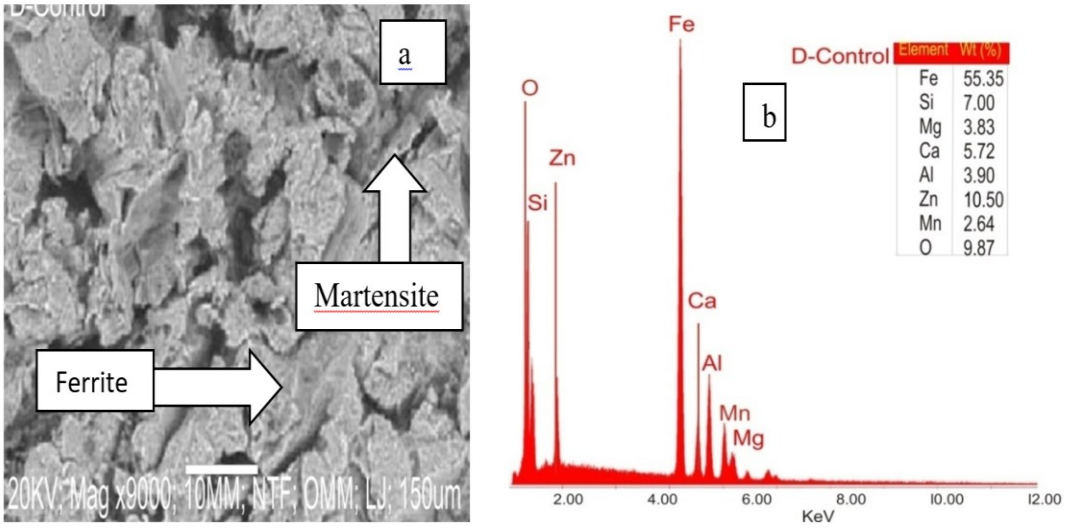


Figure 6: Sample A Control)

Due to retained austenite's transition into martensite or bainite over time, Figure 7a shows a decrease in the amount of retained austenite. Upon quenching, a portion of the austenite will persist, and upon tempering, carbon atoms will permeate from the martensite to the residual austenite, so generating a stable portion of the carbon-rich austenite. However, as a result of the deformation, the microstructure is enhanced, and the interaction between the martensite and the austenite that has been maintained causes the microstructure to restrict each phase, maintaining the stability of the austenite and this is in line with Peng *et al.,* (2021).

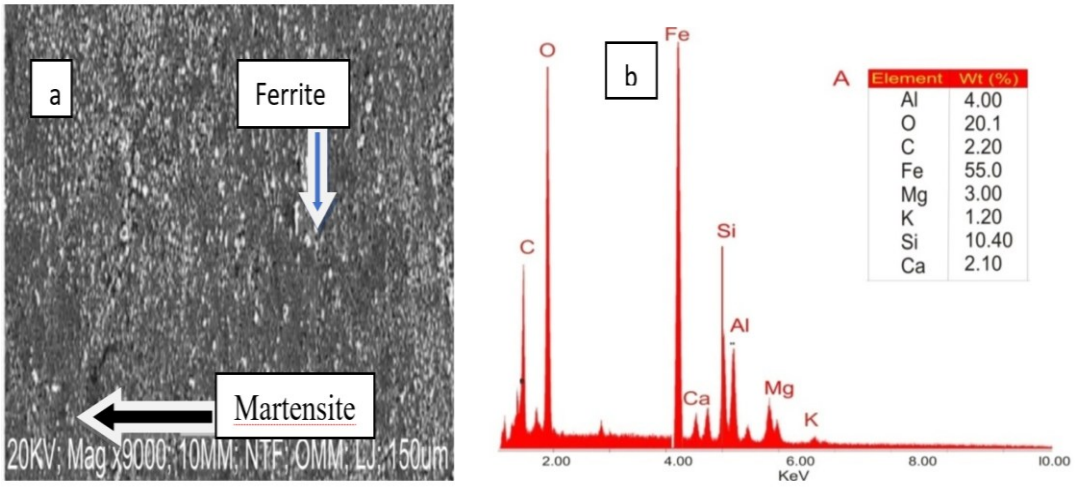


Figure 7: Sample B (743°C)

When martensite is tempered, it changes into cementite and lower carbon martensite. As can be seen in Figure 8a, the cementite that is precipitated by the rich C atoms in the martensite acquired after quenching is primarily in the form of a plate with a fairly large proportion at this tempering temperature because they will primarily form precipitates at the contact area of martensite lath throughout tempering. The fracture behavior of the second phase has a significant impact on ductility, according to recent correlation studies of the microstructures and mechanical characteristics of high strength steels with a heterogeneous structure formed via phase transformation (Leiro, 2014). The sample shows that the tempered martensite is the black area, the cementite, gray matrix area and the white spots are the ferrite.

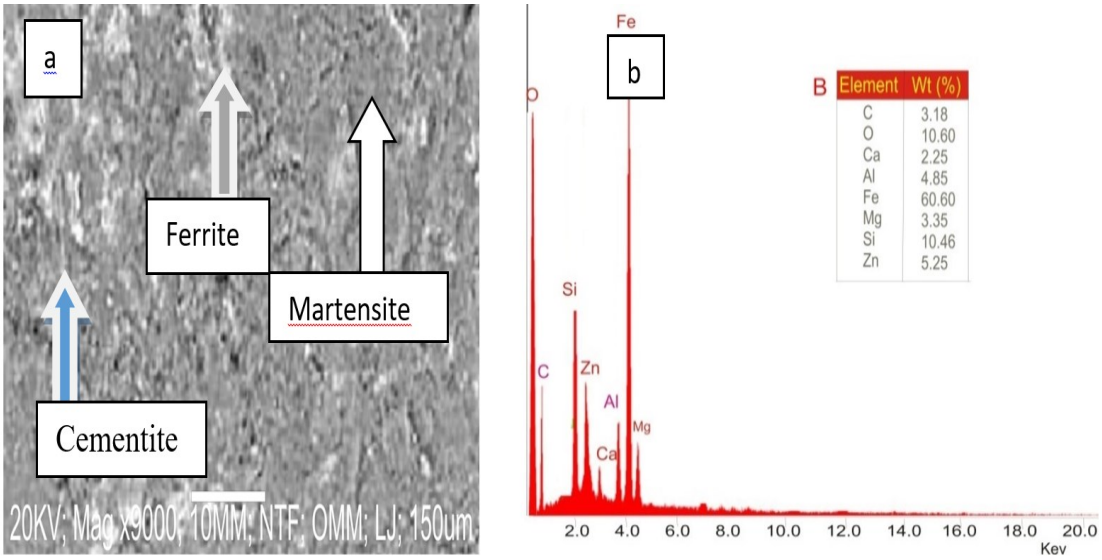


Figure 8: Sample C (761°C)

In Figure 9a, there are noticeable small-sized dimples with little quasi-cleavage facets (QCF) and short tear ridges that offer good ductility under impact force. In other words, the steels treated by heat treatment sample D displayed a clearly defined dimple pattern According to Unueroh *et al*, (2013) and Unueroh et al, (2019), the microstructure's observation of certain impurities in the steel may have contributed to the formation of fracture cracks. These results are in good agreement with the works of Hafeez *et al*., (2020) and Ren *et al.,* (2023). Greater number of tear ridges indicates higher impact absorption energy (Liu *et al*., 2014; Liu et al., 2019)

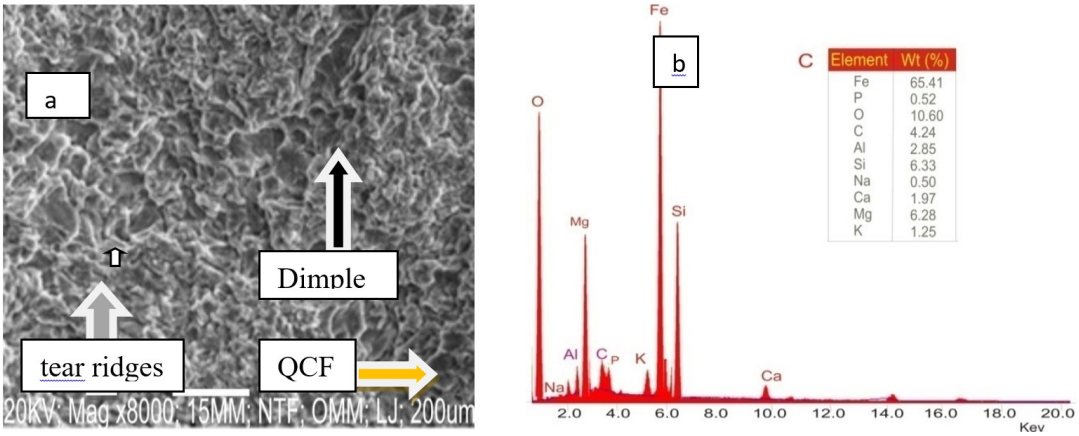


Figure 9: Sample D (779°C)

Conclusion

This study examined the mechanical properties and microstructural characteristics of martensitic steel developed via thermal cycling treatment. Following were the conclusions drawn from the findings.

i. These findings indicate that Thermal Cycling Treatment is an effective method for producing high-performance Martensitic Steel with improved mechanical properties.

ii. The mechanical properties are influenced by increase in the lamilarization temperature. At 779°C, the ultimate tensile strength, yield strength, hardnes, percentage elongation, and modulus of elasticity of the specimens increased to 610.74 MPa, 433.33 MPa, 163.49 BHN , 0.82, and 3334.43 MPa respectively, while the fracture strength and impact strength decreased to 405.70 MPa and 2.73 J/mm^2 respectively. These results suggest an increase in ductility and toughness, which enhanced the performance and formability of the tested steel.

iii. The optical micrographs of the samples tempered at 450°C showed fine-grain size and distribution of carbide (cementite), martensite, and ferrite, resulting in improved mechanical properties. Additionally, The SEM micrographs of the fracture surface revealed a considerable number of small rip ridges with superior impact absorption energy in addition to a sizable number of huge dimples with low QCF, suggesting ductile behavior.

References

A. Leiro, (2014) "Microstructure analysis of wear and fatigue in austempered high-Si steels", Doctoral thesis, Luleå University of Technology, Sweden, ISBN 978-91-7439- 885-4

Abbasi, E., Luo, Q., and Owens, D., (2018). A comparison of Microstructure and Mechanical Properties of Low-Alloy-Medium-Carbon Steels after quench-hardening Materials Science and Engineering A 725 65–75

An, H., Bao, Y., Wang, M., Yang, Q., and Huang, Y.(2019). Improvement of centre segregation in continuous casting bloom and the resulting carbide homogeneity in bearing steel GCr15 Ironmak Steelmak 46 896–905, https://doi.org/10.1080/ 03019233.2019.1604614

Antonio Augusto Gorni, (2019) Steel Forming and Heat Treating Handbook, Socorro SP Brazil, p 2 agorni@iron.com.br www.gorni.eng.br

E.P. Bagliani, M.J. Santofimia, L. Zhao, J. Sietsma, E. Anelli, (2013) Microstructure, tensile and toughness properties after quenching and partitioning treatments of a mediumcarbon steel, Mater. Sci. Eng A 559, 486–495

G. Mandal, S.K. Ghosh, S. Bera, S. Mukherjee, (2016) Effect of partial and full austenitisation on microstructure and mechanical properties of quenching and partitioning steel, Mater. Sci. Eng. A 676, 56–64

Gao, G. Gao, B. Gui, X Hu, J. He, J. Tan, Z. and Bai, B. (2019), Correlation between microstructure andyield strength of as-quenched and Q &P steels with different carbon content (0.06–0.42 wt%C Materials Science & Engineering A 753 1–10, https://doi.org/10.1016/j.msea.2019.03.018

Hafeez, M. A. Inam A. and Farooq, A. (2020), Mechanical and corrosion properties of medium carbon low alloy steel after cyclic quenching and tempering heat–treatments, Material Research Express, 7 016553, https://doi.org/10.1088/2053-1591/ab6581.

Hongli Wang, Jian Zhang, Jingtao Huang, Chengchuan Wu, Xianguang Zhang, Zhonghong Lai, Yong Liu, and Jingchuan Zhu (2023). The Evolution of a Microstructure during Tempering and Its Influence on the Mechanical Properties of AerMet 100 Steel, Journal of Materials 2023, 16, 6907

Hu, J. Du, L.X. Liu, H. Sun, G.S. Xie, H. Yi, H.L. et al., (2015), Structure–Mechanical Property relationship in a low-C Medium-Mn ultrahigh Strength heavy plate Steel with Austenite- Martensite Submicro-Laminate Structure, Mater. Sci. Eng., A 647 144–151.

Hu, J. Du, L.X. Ma, Y.N. Sun, G.S. Xie, H. and Misra, R.D.K. (2015), Effect of microalloying with molybdenum and boron on the microstructure and mechanical properties of ultralow C Ti bearing steel, Mater. Sci. Eng., A 640 259–266

Huihui Huang, Gengwei Yanga, Gang Zhao, (2018) Effect of Nb on the microstructure and properties of Ti-Mo microalloyed high-strength ferritic steel, Mater. Sci. Eng., A 736 (2018) 148–155.

Ji, Y. Tang, H. Lan, P. Shang, C. and Zhang, J. (2017), Effect of dendritic morphology and central segregation of billet castings on the microstructure and mechanical property of hot-rolled wire rods, Steel Res. Int. 88, https://doi.org/ 10.1002/srin.201600426, 1600426(1–14.

Krauss, G. (2016), Martensite in steel: strength and structure, Mater. Sci. Eng., A 273–275 40–57

Krauss, G., (2017). Tempering of Lath Martensite in Low and Medium Carbon Steels, Assessment and Challenges, steel research int. 87 No. 9999, DOI:10.1002/srin.201700038

Krolicka, A., Radwanski, K., Ambroziak, A., and Zak, A., (2019). Analysis of grain growth and Morphology of bainite in medium-carbon spring steel, Mater Sci. Eng. A. 768 138446 https://doi.org/10.1016/j.msea.138446

Lei Cheng, Qingwu Cai, Wei Yu, (2018) Coarsening of nanoscale (Ti,Mo)C precipitates in different ferritic matrixes, Mater. Char. 142 195–202

Liu J, Yu H, Zhou T, Song C and Zhang K (2014) Effect of double quenching and tempering heat treatment on the microstructure and mechanical properties of a novel 5Cr steel processed by electro-slag casting Materials Science and Engineering A619 212–20

Liu X, Xiao L, Wei C, Xu X, Luo M and Yan W. (2018). Effect of multi-directional forging and annealing on abrasive wear behavior in a medium carbon low alloy steel Tribol. Int. 119 608–13

Liu, Y., Kang, L., & Ge, H (2019) Experimental and numerical study on ductile fracture of structural steels under different stress states Journal of Constructional Steel Research, 158*, 381–404.* doi:10.1016/j.jcsr.2019.04.001

Loto R T. and Loto C A.(2019). Data on the corrosion inhibition properties of centrimonium bromide with thiocarbanilide and with vanillin on low carbon steel in dilute acid media Chemical Data Collections 22 100250–15

Ma, X. Li, X. and Langelier, B. (2018), Effects of carbon variation on microstructure evolution in weld heat-affected zone of Nb-Ti microalloyed steels, Metall. Mater. Trans. A 49 4824–4832

Majd M T, Shahrabi T and Ramezanzadeh B 2019 Low carbon steel surface modification by an effective corrosion protective nano composite film based on neodymium-polyacrylic acid benzimidazole J. Alloys Compd. 783 952–68 .

Neog, S. P., Bakshi, S. D., & Das, S. (2021). Effect of normal loading on microstructural evolution and sliding wear behaviour of novel continuously cooled carbide free bainitic steel Tribology International*, 157, 106846* doi:10.1016/j.triboint.2020.10684

Qichao Ren, Ziming Kou, Juan Wu, Tengyan Hou and Peng Xu, (2023)Effect of Tempering Temperature on Microstructure and Mechanical Properties of 35CrMo Steel, Metals 13, 771. https://doi.org/10.3390/met13040771

R. Suresh (2021) Investigation of Heat Treatment on Mechanical Properties of Medium Carbon Steel. International Journal of Scientific Research in Science, Engineering and Technology Print ISSN: 2395- 1990 Online ISSN: 2394-4099 doihttps://doi.org/10.32628/IJSRSET21868

Shu, Z.Q.; Yuan, P.B.; Ouyang, Z.Y.; Gong, D.M.; Bai, X.M.(2017**)** Effects of Tempering Temperature on Microstructure and Mechanical Properties of Drill Pipe Steel 26CrMo. Acta Metall Sin 53, 669–676.

Singh, P.; Singh, S.(2021) Effect of quenching media on microstructural evolution, mechanical and wear properties of AISI4135 steel Proc. Inst. Mech. Eng. Part C J. Mech. Eng. Sci.235, 5616–5625

Tao, X. Li, C. Han, L. and Gu, J., (2016). Microstructure evolution and mechanical properties of X12CrMoWVNbN10-1-1 steel during quenching and tempering processJournal of Materials Research and Technology 5 45–57 Technology, Vol 162, p223-249

Unueroh Ufuoma Georgina, Igbinomwanhia Noel Osabuohien (2019). Effect of Austenising Temperature on the Tensile Property of AISI 1040 Steel, Journal of Science and Technology Research 1(3) pp. 50-57 ISSN-2682-5821

Unueroh UG, Onyekpe BO. (2013) Effect of austenising temperature on the tensile property of AISI 1040 steel, International Journal of Material Science Innovations (IJMSI) 1 (4): 182-191, ISSN 2289-4063

Villalobos J C, Serna S A, Campillo B and Martınez E L (2016), Evaluation of mechanical properties of an experimental micro-alloyed steel subjected to tempering heat treatment and its effect on hydrogen embrittlement Int. J. Hydrogen Energy 42 689–98

Wang C, Qiu H, Kimura Y and Inoue T (2016), Morphology, crystallography, and crack paths of tempered lath martensite in a medium carbon low alloy steel Materials Science and Engineering A 669 48–57

Yan Peng*, Caiyi Liu and Ningning Wang, (2021)Efect of Deformation on Microstructure and Mechanical Properties of Medium Carbon Steel During Heat Treatment Process, Chinese Journal of Mechanical Engineering (2021) 34:113, https://doi.org/10.1186/s10033-021-00634-8

Zhang Y, Zhan D, Qi X, Jiang Z and Zhang H (2017) Microstructure and mechanical properties of Cr14 ultra-high-strength steel at different tempering temperatures around 773 Materials Science and Engineering A 698 152–61

Zhou, S. Tong, Li, Z. dong Yang, C. fu, Xie, S. kun, and Yong, Q. long. (2019), Cleavage fracture and microstructural effects on the toughness of a medium carbon pearlitic steel for high-

Zhou, X. Shao, Z Tian, F. Hopper, C. and Jiang, J. (2020), Microstructural effects on central Crack formation in hot cross-wedge-rolled high-strength steel parts, J. Mater. Sci.55 9608–9622, https://doi.org/10.1007/s10853-020-04677-5